Article

Light-Induced Excited-State Spin Trapping in Tetrazole-Based Spin Crossover Systems

Bele#n Ordejo#n, Coen de Graaf, and Carmen Sousa

J. Am. Chem. Soc., **2008**, 130 (42), 13961-13968 • DOI: 10.1021/ja804506h • Publication Date (Web): 24 September 2008

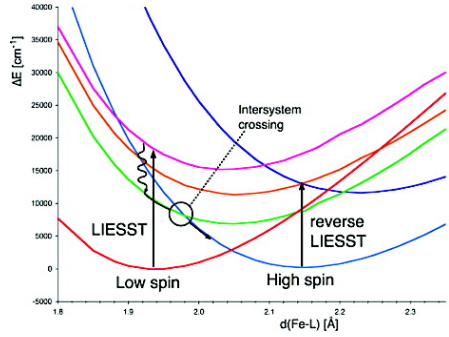

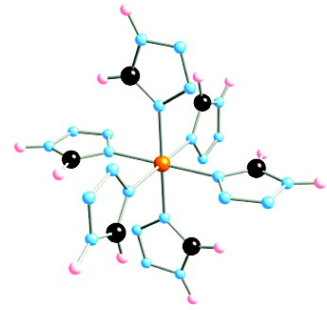

More About This Article

Additional resources and features associated with this article are available within the HTML version:

- Supporting Information
- Access to high resolution figures
- Links to articles and content related to this article
- Copyright permission to reproduce figures and/or text from this article

View the Full Text HTML

J|A|C|S
ARTICLES

Published on Web 09/24/2008

Light-Induced Excited-State Spin Trapping in Tetrazole-Based Spin Crossover Systems

Belén Ordejón,[†] Coen de Graaf,*[,†,‡] and Carmen Sousa[§]

Departament de Química Física i Inorgànica, Universitat Rovira i Virgili, Marcel-lí Domingo s/n, 43007 Tarragona, Spain, Institució Catalana de Recerca i Estudis Avançats (ICREA), Passeig Lluís Companys 23, 08010 Barcelona, Spain, and Departament de Química Física and Institut de Química Teòrica i Computacional (IQTCUB), Universitat de Barcelona, C/Martí i Franquès 1, 08028 Barcelona, Spain

Received June 13, 2008; E-mail: coen.degraaf@urv.cat

Abstract: Ab initio calculations have been performed on $Fe^{II}(tz)_6$ (tz = 1-*H*-tetrazole) to establish the variation of the energy of the electronic states relevant to (reverse) light-induced excited-state spin trapping (LIESST) as function of the Fe−ligand distance. Equilibrium distances and absorption energies are correctly reproduced. The deactivation of the excited singlet is proposed to occur in the Franck−Condon region through overlap of vibrational states with an intermediate triplet state or an intersystem crossing along an asymmetric vibrational mode. This is followed by an intersystem crossing with the quintet state. Reverse LIESST involves a quintet−triplet and a triplet−singlet intersystem crossing around the equilibrium distance of the high-spin state. The influence of the transition metal is studied by changing Fe^{II} for Co^{II}, Co^{III}, and Fe^{III}. The calculated curves for Fe^{III} show remarkable similarity with Fe^{II}, indicating that the LIESST mechanism is based on the same electronic conversions in both systems.

1. Introduction

A new challenge in the area of molecular magnetism is the design of optically switchable magnetic materials. The potentially interesting magnetic materials need to exhibit bistability between two (or more) different spin states. The interconversion between the different spin states, called spin crossover phenomenon, can be triggered by a change in temperature, pressure, or irradiation with light, being the latter the most appealing phenomenon for technical applications. Spin crossover behavior may be observed in compounds with transition metals of the first series with $3d^4$ to $3d^7$ electron configurations and can be explained qualitatively by ligand-field theory.[1] The electronic ground-state of such complexes is either the high-spin (HS) state at low ligand-field strength or the low-spin state (LS) at high ligand-field strength. Spin crossover compounds show an LS ground-state at low temperatures with a zero-point energy difference between the HS and LS states (ΔE^0_{HL}) typically of the order of 0−2000 cm^{-1}.[1,2] Usually, the LS to HS spin transition is accompanied by a substantial elongation of the metal−ligand bond lengths. A large number of spin crossover complexes known up to now contains Fe^{II} in a $3d^6$ electronic configuration and a N_6 first coordination sphere. For these compounds, the change in the Fe−N distances from the LS to the HS state is found to be typically ∼0.2 Å.[1]

The spin conversion from LS to HS states can be optically triggered by photoirradiation based on the light-induced excited-spin state trapping (LIESST) phenomenon.[3−6] In fact, LIESST has been initially discovered for six-coordinated Fe^{II} complexes, and its mechanism has been elucidated by Hauser.[5] It is believed that LIESST occurs through spin-allowed excitations from the LS state into d−d or ligand−metal charge transfer (LMCT) bands followed by a double intersystem crossing involving an intermediate spin state. For instance, if an LS Fe^{II} sample is irradiated with green light at low temperatures, the $^1A_1 \rightarrow {}^1T_1$ or $^1T_2$ excitation promotes a quantitative conversion to the metastable $^5T_2$ HS state, where the system remains trapped with a large lifetime. This conversion takes place via an intermediate $^3T_1$ or $^3T_2$ state.

It is important to realize that the two intersystem crossings, from the populated singlet excited-state to the intermediate triplet state and from the triplet to the lowest quintet state, and therefore the whole LIESST process, are only possible because of the spin−orbit coupling. It has also been shown in some materials that the process can be reversible, i.e., a light-induced HS → LS reconversion is possible by irradiating the sample with red light, thus promoting a $^5T_2 \rightarrow {}^5E$ absorption. Again through two intersystem crossings involving triplet states, the LS state can be populated. Clearly, the LIESST phenomenon found in Fe^{II} spin crossover materials contains the basic properties

[†] Universitat Rovira i Virgili.
[‡] Institució Catalana de Recerca i Estudis Avançats (ICREA).
[§] Universitat de Barcelona.

(1) Hauser, A. In *Spin crossover in Transition Metal Compounds I*; Gütlich P., Goodwin H. A., Eds.; Topics in Current Chemistry; Springer-Verlag: Berlin, 2004; Vol. 233, p 49.
(2) Gütlich, P.; Goodwin, H. A. In *Spin crossover in Transition Metal Compounds I*; Gütlich P., Goodwin H. A., Eds.; Topics in Current Chemistry; Springer-Verlag: Berlin, 2004; Vol. 233, p 1.
(3) Decurtins, S.; Gütlich, P.; Kohler, C. P.; Spiering, H.; Hauser, A. *Chem. Phys. Lett.* **1984**, *105*, 1–4.
(4) Decurtins, S.; Gütlich, P.; Kohler, C. P.; Spiering, H. *J. Chem. Soc., Chem. Commun.* **1985**, 430–432.
(5) Hauser, A. *J. Chem. Phys.* **1991**, *94*, 2741–2748.
(6) Hauser, A. In *Spin crossover in Transition Metal Compounds II*; Gütlich P., Goodwin H. A., Eds.; Topics in Current Chemistry; Springer-Verlag: Berlin, 2004; Vol. 234, p 155.

required for all optical data storage and processing devices. However the HS → LS relaxation, due to thermal activation at elevated temperatures and tunneling processes at temperatures below ≈50 K, prohibits its potential applications in such devices.[7−9] To minimize the thermal and tunneling processes, and therefore to increase the probability of LIESST to occur, the geometrical differences between the LS and HS states must be large; their energy difference, ΔE^0_{HL}, must be small; and the energy barrier for the HS → LS relaxation must be larger than ΔE^0_{HL}. For a long time, it was believed that the LIESST phenomenon was strictly limited to Fe^{II} complexes[6] since the bond length difference for Fe^{III} compounds upon spin crossover (typically 0.15 Å) is smaller than in Fe^{II} complexes, resulting in a much larger tunneling rate constant at low temperatures for the former.[10,11] However, experimental evidence has recently been reported showing that the LIESST process is also possible for Fe^{III} systems.[12−14] Nevertheless, the underlying mechanism remains unclear.

Although a qualitative description of the electronic structure of spin crossover compounds can be reached by ligand-field theory,[1] this theory does not provide quantitative accuracy to obtain the key parameters of spin crossover materials. Hence, a comprehensive theoretical study of the electronic structure is needed to understand the photophysical properties of spin crossover systems. Despite the enormous impact of spin crossover and related phenomena such as LIESST, there are relatively few studies in the literature addressing these phenomena from a computational point of view. In a pioneering work, Paulsen and collaborators applied density functional theory (DFT) calculations to investigate the molecular geometry, Mössbauer parameters, vibration frequencies and entropy differences between HS and LS states in various spin crossover systems.[15−17] Although these methods give a fairly accurate description of these properties, the precision is not sufficient to reach a correct estimation of ΔE^0_{HL}. This parameter is clearly one of the most important and yet most difficult to calculate in the field of spin crossover materials. In fact, many of the theoretical works of Fe^{II} complexes are focused on the relative stabilities of the LS and HS states. Most of the computational studies published are based on DFT calculations employing different exchange and correlation functionals. It is shown that the choice of the exchange functional is critical on calculating the relative energies between the possible spin states, being the correlation functional less important.[18] In general, pure DFT methods favor the LS ground-state leading to too large ΔE^0_{HL} while hybrid functionals like B3LYP give better values but tend to overstabilize high-spin states.[15,19,20] Several studies have been performed to establish the optimal percentage of exact exchange in hybrid functionals. Nevertheless, results show that it ranges between 10−25% depending on the particular system.[21−25] An alternative way to estimate ΔE^0_{HL} with DFT-based computational schemes has recently been presented.[26] This indirect calculation of the HS−LS energy difference is based on the computation of differences of the vertical HS−LS energy gaps at different geometries and turns out to be almost independent of the choice of functional.

Only few works using wave function based methods have been reported because these are computationally much more demanding than DFT. Spectroscopy-oriented configuration interaction (SORCI)[27] and multiconfigurational second-order perturbation theory (CASPT2)[28] have been applied to six-coordinated Fe^{II} complexes with various ligands.[20,22,29] Results showed that using sufficiently large basis sets accuracy within 1000 cm^{-1} can be achieved.

To get detailed insight into the LIESST phenomena, it is necessary to study not only the LS ground-state and the low-lying HS state but also the potential energy surfaces of all relevant excited spin states that could be involved in the mechanism. However, assessment of excited states is a difficult task and for this reason theoretical investigations of the LIESST mechanism are very scarce. Only Ando et al.[30] have recently reported potential energy surfaces for a Fe^{III} complex by means of DFT calculations using the B3LYP functional. The study was limited to the lowest HS (sextet), LS (doublet), and intermediate spin state (quartet) potential energy surfaces, whereas the vertical absorption bands from the doublet or the sextet electronic states to the excited states were estimated by time-dependent DFT (TD-DFT) calculations. Singlet to singlet vertical excitations on the $[Fe(ptz)_6]^{2+}$ cation have also been studied by TD-DFT within the B3LYP funtional by Rodriguez.[31] On the other hand, Kondo et al.[32] in a study of an Fe^{II} spin crossover system estimated the strength of the spin−orbit coupling between the singlet and triplet states and between the triplet and quintet states. Despite the fact that these authors did not compute the spin−orbit coupling at the crossing between the relevant potential energy surfaces but at the optimized geometry corresponding to the lowest singlet and quintet states, they concluded that the $^3T_2$ intermediate state can play a significant role in the (reverse) LIESST process.

(7) Hauser, A. *Coord. Chem. Rev.* **1991**, *111*, 275–290.
(8) Hauser, A.; Vef, A.; Adler, P. *J. Chem. Phys.* **1991**, *95*, 8710–8717.
(9) Buhks, E.; Bixon, M.; Jortner, J. *J. Am. Chem. Soc.* **1980**, *102*, 2918–2923.
(10) Schenker, S.; Hauser, A. *J. Am. Chem. Soc.* **1994**, *116*, 5497–5498.
(11) Schenker, S.; Hauser, A.; Dyson, R. M. *Inorg. Chem.* **1996**, *35*, 4676–4682.
(12) Hayami, S.; Gu, Z.-z.; Shiro, M.; Einaga, Y.; Fujishima, A.; Sato, O *J. Am. Chem. Soc.* **2000**, *122*, 7126–7127.
(13) Juhasz, G.; Hayami, S.; Sato, O.; Maeda, Y. *Chem. Phys. Lett.* **2002**, *364*, 164–170.
(14) Sato, O. *Acc. Chem. Res.* **2003**, *36*, 692–700.
(15) Paulsen, H.; Trautwein, A. X. In *Spin crossover in Transition Metal Compounds III*; Gütlich, P., Goodwin, H. A., Eds.; Topics in Current Chemistry; Springer-Verlag: Berlin, 2004; Vol. 235, p 197.
(16) Paulsen, H.; Duelund, L.; Winkler, H.; Toftlund, H.; Trautwein, A. X. *Inorg. Chem.* **2001**, *40*, 2201–2203.
(17) Paulsen, H.; Benda, R.; Herta, C.; Schünemann, V.; Chumakov, A. I.; Duelund, L.; Winkler, H.; Toftlund, H.; Trautwein, A. X. *Phys. Rev. Lett.* **2001**, *86*, 1351–1354.
(18) Swart, M.; Groenhof, A. R.; Ehlers, A. W.; Lammertsma, K. *J. Phys. Chem. A* **2004**, *108*, 5479–5483.
(19) Simaan, A. J.; Boillot, M. L.; Carrasco, R.; Cano, J.; Girerd, J. J.; Mattioli, T. A.; Ensling, J.; Spiering, H.; Gütlich, P. *Chem.—Eur. J.* **2005**, *11*, 1779–1793.
(20) Pierloot, K.; Vancoillie, S. *J. Chem. Phys.* **2006**, *125*, 124303.
(21) Fouqueau, A.; Mer, S.; Casida, M. E.; Lawson, L. M.; Hauser, A. *J. Chem. Phys.* **2004**, *120*, 9473–9486.
(22) Fouqueau, A.; Casida, M. E.; Lawson, L. M.; Hauser, A.; Neese, F. *J. Chem. Phys.* **2005**, *122*, 044110.
(23) Lawson Daku, L. M.; Vargas, A.; Hauser, A.; Fouqueau, A.; Casida, M. E. *ChemPhysChem* **2005**, *6*, 1393–1410.
(24) Reiher, M. *Inorg. Chem.* **2002**, *41*, 6928–6935.
(25) Scherlis, D. A.; Estrin, D. A *Int. J. Quantum Chem.* **2002**, *87*, 158–166.
(26) Zein, S.; Borshch, S. A.; Fleurat-Lessard, P.; Casida, M. E.; Chermette, H. *J. Chem. Phys.* **2007**, *126*, 014105.
(27) Neese, F. *J. Chem. Phys.* **2003**, *119*, 9428–9443.
(28) Andersson, K.; Malmqvist, P.-Å.; Roos, B. O *J. Chem. Phys.* **1992**, *96*, 1218–1226.
(29) Pierloot, K.; Vancoillie, S. *J. Chem. Phys.* **2008**, *128*, 034104.
(30) Ando, H.; Nakao, Y.; Sato, H.; Sakaki, S. *J. Phys. Chem. A* **2007**, *111*, 5515–5522.
(31) Rodriguez, J. H. *J. Chem. Phys.* **2005**, *123*, 094709.
(32) Kondo, M.; Yoshizawa, K. *Chem. Phys. Lett.* **2003**, *372*, 519–523.

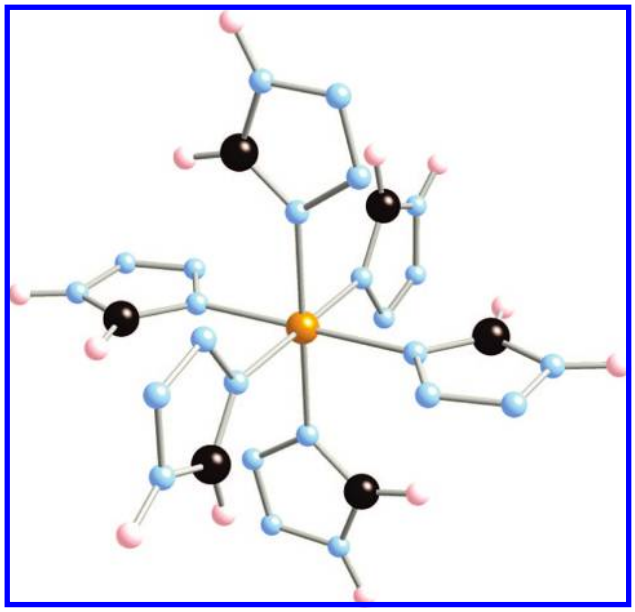

Figure 1. Ball and stick representation of the model $TM(tz)_6$ complex. Black spheres represent C, blue N, and pink H. The central sphere represents the TM.

In this work, we aim to achieve an accurate description of the microscopic properties of spin crossover systems and to understand the basic mechanism of LIESST by wave function based electronic structure calculations. The complete active space self-consistent field (CASSCF)/CASPT2 approach adopted here includes the three essential ingredients for this purpose: (i) a proper description of the spin of the various electronic states involved in the proccess, (ii) a direct access to excited states, which can be treated at the same footing as the ground state, and (iii) the inclusion of spin−orbit effects, which are important to explain the intersystem crossings.

Since many of the spin crossover systems found to date contain a FeN_6 core, where the N atom is preferably arranged in an aromatic system, we choose a model compound formed by an Fe^{II} ion coordinated by six tetrazole ligands, $[Fe(tz)_6]^{2+}$. This system can be thought of as a simplified representation of the $Fe(mtz)_6(BF_4)_2$ and $Fe(ptz)_6(BF_4)_2$ spin crossover compounds (mtz = 1-methyltetrazole and ptz = 1-propyltetrazole). Although spin crossover phenomena may be influenced by the crystalline environment,[33] the essential ingredients for LIESST are present in our isolated model compound, illustrated by the fact that LIESST has also been observed for molecules in solution.[34]

Moreover, we have considered the effect of changing the transition metal on the structural and electronic properties related to the spin crossover process. Therefore, in addition to the $[Fe(tz)_6]^{2+}$ complex with Fe^{II}-$3d^6$, we have studied the isoelectronic $[Co^{III}(tz)_6]^{3+}$ system. As LIESST has been recently found in Fe^{III} compounds, we have also analyzed the $[Fe(tz)_6]^{3+}$ model system, where the iron ion has a $3d^5$ electronic configuration. Finally, the possibility of finding thermal spin crossover and/or LIESST on Co^{II} systems have been analyzed by studying the $[Co(tz)_6]^{2+}$ complex, where the electronic configuration of the TM is $3d^7$.

(33) Yamada, M.; Hagiwara, H.; Torigoe, H.; Matsumoto, N.; Kojima, M.; Dahan, F.; Tuchagaes, J.-P.; Re, N.; Iijima, S. *Chem.—Eur. J.* **2006**, 4536–4549.
(34) McGarvey, J. J.; Lawthers, I. *J. Chem. Soc., Chem. Commun.* **1982**, 906–907.

2. Methodology

All calculations were performed applying the CASSCF/CASPT2[28] method implemented in MOLCAS 7.0.[35] Although this methodology has also been used to investigate ground-state properties, it is unique in its ability to accurately describe excited states. Since its development in the early 1990s, this method has been successfully applied to the interpretation of spectroscopic data in a wide range of compounds including organic molecules,[36−38] transition metal materials,[39−42] and recently also systems containing lanthanides or actinides.[43−45] Nowadays the method is also regularly applied to photochemical processes.[46−49] The first part of the calculations produces a high-quality reference wave function for the subsequent perturbational treatment of the remaining (mainly atomic) electron correlation effects through CASPT2. Scalar relativistic effects are included using a Douglas−Kroll−Hess Hamiltonian.[50] The treatment of the spin−orbit effects is based on the spin−orbit state interaction (SO-SI) approach.[51−53] The spin−orbit Hamiltonian is constructed in the space spanned by the CASSCF wave funtions of the relevant spin-free electronic states. The diagonal elements of this Hamiltonian are modified to account for dynamical correlation effects by replacing the CASSCF energies with the CASPT2 values. Within this approximation, it is implicitly assumed that spin−orbit coupling and electron correlation effects are largely decoupled.

The Fe and Co tetrazole complexes were constructed as follows: First, the geometry of an isolated tetrazole ligand (L) was optimized at the CASPT2 level. The resulting interatomic distances and angles are in good agreement with the experimental values.[58] In a second step, the Fe or Co atom was surrounded by six optimized tetrazole ligands in an octahedral coordination (see Figure 1). The local symmetry around the transition metal (TM) shows an inversion center, as in the crystal structure of the $Fe(mtz)_6(BF_4)_2$ and $Fe(ptz)_6(BF_4)_2$ spin crossover compounds. The torsion angle of the tetrazole rings were kept to zero, although in the experimental structures it varies between 5° and 15°. However, exploratory calculations show that the dependence of the energy on this degree of freedom is weak. To evaluate the potential energy surfaces (PES) of the relevant electronic states, the internal coordinates of the

(35) Karlström, G.; Lindh, R.; Malmqvist, P.-Å.; Roos, B. O.; Ryde, U.; Veryazov, V.; Widmark, P.-O.; Cossi, M.; Schimmelpfennig, B.; Neograd, P.; Seijo, L. *Comput. Mater. Sci.* **2003**, *28*, 222–239.
(36) Serrano-Andrés, L.; Merchán, M. *J. Mol. Struct. (Theochem)* **2005**, *729*, 99–108.
(37) Corral, I.; Gonzalez, L.; Lauer, A.; Freyer, W.; Fidder, H.; Heyne, K. *Chem. Phys. Lett.* **2008**, *452*, 67–71.
(38) Roos, B. O.; Malmqvist, P.-Å.; Molina, V.; Serrano-Andrés, L.; Merchán, M. *J. Chem. Phys.* **2002**, *116*, 7526–7536.
(39) Pierloot, K.; De Kerpel, J.; Ryde, U.; Olsson, M. H. M.; Roos, B. O. *J. Am. Chem. Soc.* **1998**, *120*, 13156–13166.
(40) Sousa, C.; de Graaf, C.; Illas, F.; Barriuso, M. T.; Aramburu, J. A.; Moreno, M. *Phys. Rev. B* **2000**, *62*, 13366–13375.
(41) de Graaf, C.; Sousa, C.; de P. R.; Moreira, I.; Illas, F *J. Phys. Chem. A* **2001**, *105*, 11371–11378.
(42) Brynda, M.; Gagliardi, L.; Widmark, P.-O.; Power, P. P.; Roos, B. O. *Angew. Chem., Int. Ed.* **2006**, *45*, 3804–3807.
(43) Ordejón, B.; Seijo, L.; Barandiarán, Z. *J. Chem. Phys.* **2007**, *126*, 194712.
(44) Gagliardi, L.; Roos, B. O. *Chem. Soc. Rev.* **2007**, 36.
(45) Roos, B. O.; Malmqvist, P.-Å.; Gagliardi, L. *J. Am. Chem. Soc.* **2006**, *128*, 17000–17006.
(46) Serrano-Andrés, L.; Merchán, M.; Borin, A. *J. Am. Chem. Soc.* **2008**, *130*, 2473–2484.
(47) Blancafort, L.; Migani, A. *J. Am. Chem. Soc.* **2007**, *129*, 14540–14541.
(48) Martin, M. E.; Negri, F.; Olivucci, M. *J. Am. Chem. Soc.* **2004**, *126*, 5452–5464.
(49) Frutos, L. M.; Andruniów, T.; Santoro, F.; Ferré, N.; Olivucci, M. *Proc. Natl. Acad. Sci. USA* **2007**, *104*, 7764–7769.
(50) Douglas, N.; Kroll, N. M. *Ann. Phys.* **1974**, *82*, 89–155.
(51) Malmqvist, P.-Å.; Roos, B. O.; Schimmelpfennig, B *Chem. Phys. Lett.* **2002**, *357*, 230–240.
(52) Roos, B. O.; Malmqvist, P.-Å *Phys. Chem. Chem. Phys.* **2004**, *6*, 2919–2927.
(53) Gagliardi, L.; Roos, B. O. *Nature* **2005**, *433*, 848–851.

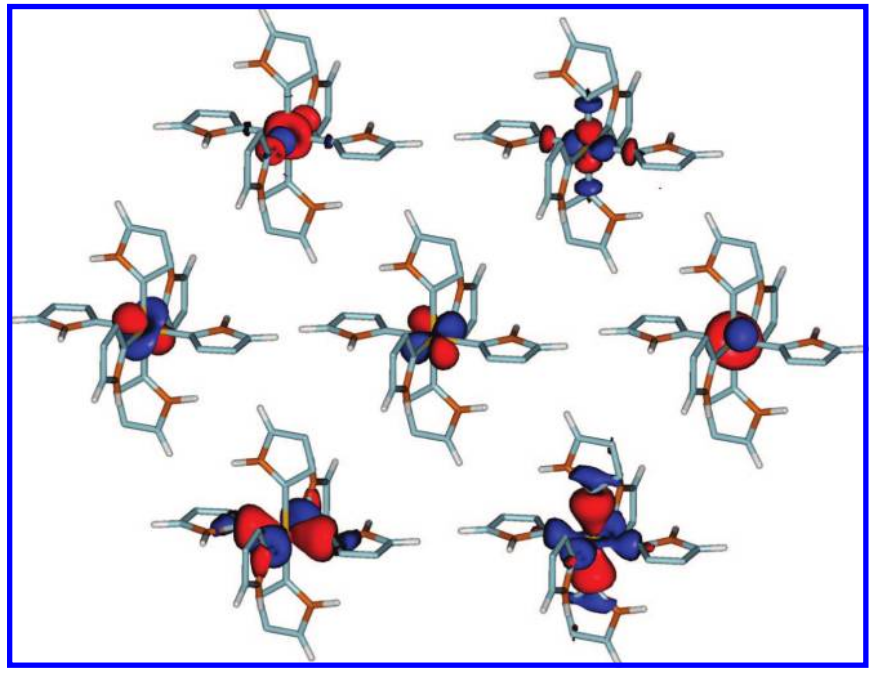

Figure 2. Fe-3d(e_g) (top), Fe-3d(t_{2g}) (middle), and L-2p(e_g) (bottom) active orbitals of $Fe^{II}(tz)_6$.

tetrazole ligands were kept frozen to the optimized CASPT2 values while the distances between the Fe or Co atoms and the N of the tetrazole ligands were symmetrically varied. Hence, the TM-N distance was chosen as reaction coordinate. This strategy is justified by the fact that crystalographic data available for the mentioned tetrazole-based spin crossover compounds[59,60] show that the main differences between the LS and HS structures come from the TM−L distances and not from the internal geometry of the ligand.

The active space and the size of the one-electron basis set has been chosen following the conclusions of a previous study of Pierloot and Vancoillie[20] The active space used to obtain the CASSCF wave functions contains 12 orbitals and, depending on the sytem, 9 (Fe^{3+}), 10 (Fe^{2+} and Co^{3+}), or 11 (Co^{2+}) electrons. The active orbitals include the five 3d Fe or Co orbitals, a second 3d shell to properly account for dynamical correlation effects of the 3d electrons,[54,55] and two e_g-like bonding ligand orbitals as shown in Figure 2. This active space gives an accurate description of the Fe-3d radial electron correlation and the LMCT effects due to the σ donation of the ligands. A further extension of the active space with ligand-π^* orbitals to incorporate a possible π-back-donation[61] in the wave function was not successful. The energy gain due to the π-back-donation turned out to be so small that the competing mechanism of Fe-3d radial correlation is more favorable and the extra orbitals in the active space become additional Fe-3d′(t_{2g}) orbitals. No changes in ΔE^0_{HL} or R_e were observed with this active space, indicating the convergence of the results with the size of the active space. CASPT2 accounts for the remaining (mainly atomic) electron correlation by correlating all the electrons except the deep core electrons (1s for C and N, 1s−2p for Fe and Co).

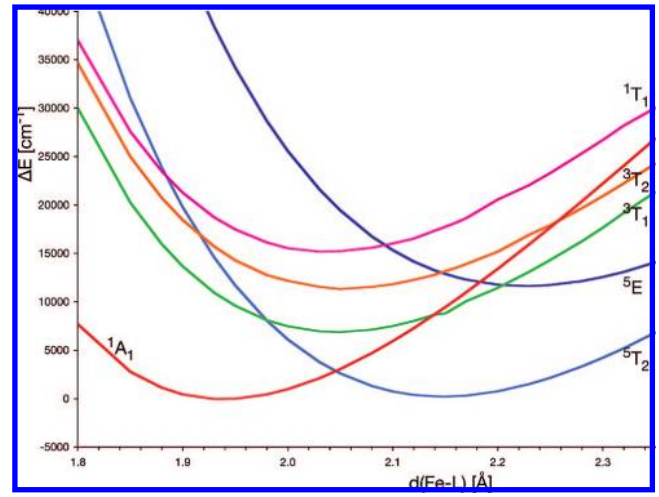

Figure 3. CASPT2 relative energies (cm^{-1}) of the low-lying singlet, triplet, and quintet states of $Fe^{II}(tz)_6$ as a function of the Fe−ligand distance.

For all atoms, the atomic natural orbital basis set have been used, specifically designed to include relativistic effects.[56,57] These basis sets were contracted as follows: a (7s, 6p, 5d, 4f, 3g, 2h) contraction for Fe and Co atoms, (4s, 3p, 1d) for the N bonded to TM, (3s, 2p) for the other N atoms and for C, and a (2s) basis set for H. A detailed validation of the method can be found in the Supporting Information.

3. Results

3.1. $Fe^{II}(tz)_6$. Figure 3 shows the dependence of the CASPT2 energies of the lowest singlet, triplet and quintet states on the Fe−ligand distance. The equilibrium distances R_e of the LS ($^1A_1$) and HS ($^5T_2$) states are 1.95 and 2.15 Å, respectively, in good agreement with the experimental values for $Fe(mtz)_6(BF_4)_2$ and $Fe(ptz)_6(BF_4)_2$ of 1.99 and 2.18 Å. The energy of the LS

(54) Andersson, K.; Roos, B. O. *Chem. Phys. Lett.* **1992**, *191*, 507–514.
(55) de Graaf, C.; Broer, R.; Nieuwpoort, W. C. *Chem. Phys.* **1996**, *208*, 35–43.
(56) Roos, B. O.; Lindh, R.; Malmqvist, P.-Å.; Veryazov, V.; Widmark, P.-O *J. Phys. Chem. A* **2005**, *109*, 6575–6579.
(57) Roos, B. O.; Lindh, R.; Malmqvist, P.-Å.; Veryazov, V.; Widmark, P.-O *J. Phys. Chem. A* **2004**, *108*, 2851–2858.
(58) Goddard, R.; Heinemann, O.; Krüger, C. *Acta Crystallogr. Sect. C* **1997**, *53*, 590–592.
(59) Kusz, J.; Spiering, H.; Gütlich, P. *J. Appl. Crystallogr.* **2000**, *33*, 201–205.
(60) Kusz, J.; Spiering, H.; Gütlich, P. *J. Appl. Crystallogr.* **2001**, *34*, 229–238.
(61) Ribas-Ariño, J.; Novoa, J. J. *Chem. Commun.* **2007**, 3160–3162.

Table 1. CASPT2 Vertical Transition Energies (cm^{-1}) in $Fe^{II}(tz)_6$ Compared to Experimental Data for $Fe^{II}(ptz)_6(BF_4)_2$

transition	CASPT2	exp[5]
$^1A_1 \rightarrow {}^1T_1$	17470	18200
$^5T_2 \rightarrow {}^5E$	12654	12200
$^1A_1 \rightarrow {}^3T_1$	9585	10280
$^1A_1 \rightarrow {}^3T_2$	14282	14300

state at R_e (LS) is slightly lower than the energy of the HS state at R_e (HS); the energy difference is -220 cm^{-1}, in agreement with the fact that the LS is the ground-state at low temperatures. A comparison with experiment requires the inclusion of the zero-point energy. The harmonic frequencies of the symmetric Fe−L vibration can be estimated from the curvature of the PES around R_e. We obtain 400 cm^{-1} for the HS state and, as expected, a slighty larger value of 480 cm^{-1} for the LS state. This results in a ΔE^0_{HL} of -180 cm^{-1}, in good agreement with the experimental estimate of -120 cm^{-1} by Hinek et al.[62] The energy barrier for HS ↔ LS relaxation is approximately 2800 cm^{-1}, which is definitely larger than ΔE^0_{HL} and sufficient to trap the system in the metastable HS state.

The spectroscopy of the tetrazole-based spin crossover systems is reproduced with high precision as shown in Table 1. The excitation energy of the first step in the LIESST process (the excitation of the system from the $^1A_1$ state into the $^1T_1$ state) is reproduced correctly, as is the initial stage of the reverse LIESST process, the $^5T_2 \rightarrow {}^5E$ excitation. This demonstrates that the potential energy curves depicted in Figure 3 give a good account of the energy dependence of the different states on the Fe−ligand distance. All the states depicted in Figure 3 are dominated by Fe-$3d^6$ electronic configurations, and hence, all excitations described in this work can be considered as d−d transitions. Other type of excitations such as ligand-to-metal or metal-to-ligand charge transfer transitions lie at higher energy in the present system.

The first observation that can be made on inspection of the ab initio potential energy curves is the existence of a $^1T_1$−$^5T_2$ intersystem crossing in the Franck−Condon region at ≈1.89 Å. This provides a direct path for the excited electron to the metastable HS state and was already mentioned by Hauser and co-workers.[7] The second observation is the fact that there is no crossing between the excited singlet and the $^3T_1$ or $^3T_2$ state. At all distances, the $^1T_1$−$^3T_2$ energy difference is between 2800 and 5700 cm^{-1}, which is significantly larger than the intrinsic precision of the CASPT2 method (∼800 cm^{-1}). These triplets do however show intersystem crossing with the $^5T_2$ state. Finally, we observe a $^1T_1$−^5E crossing near the equilibrium distance of the excited singlet state, around 2.1 Å.

To further discuss the LIESST mechanism, the inclusion of spin−orbit coupling is mandatory. Given the fact that the complex only contains relatively light elements, it is not unexpected that the influence of the spin−orbit coupling on the general shape of the curves is small, no qualitative changes in the surfaces were observed. The only place where the spin−orbit coupling has a significant effect is at the crossing points. Figure 4 zooms in on two of these crossings and shows the spin−orbit resolved energies: On the upper part, the crossing between the $^1T_1$ and the $^5T_2$ states is at 1.89 Å, and on the lower part, the $^3T_2$−$^5T_2$ crossing is at 1.92 Å. The behavior at these crossings is representative for all singlet−quintet and triplet−quintet crossings, respectively. Crystal field and spin−orbit coupling

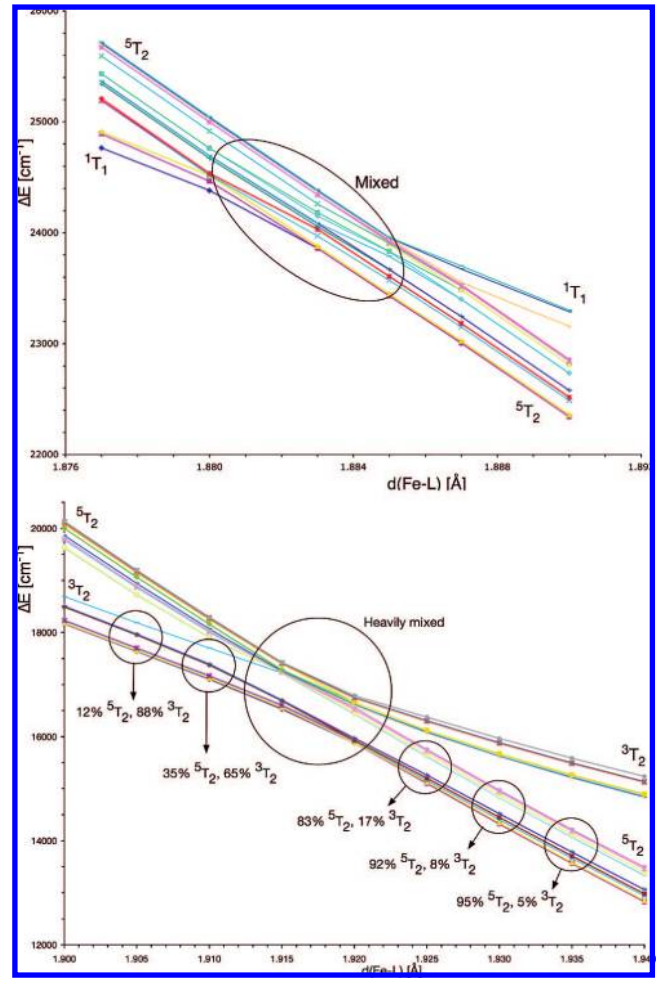

Figure 4. Relative energies (cm^{-1}) of the spin−orbit states arising from the singlet−quintet crossing around 1.89 Å (upper part) and from the triplet−quintet crossing around 1.92 Å (lower part).

give rise to 15 nondegenerate states for $^5T_2$, 9 for $^3T_2$, and 3 states for $^1T_1$. The spin−orbit resolved singlet−quintet crossing takes place in a very small distance interval of ≈0.005 Å, from 1.880 to 1.885 Å (see the top of Figure 4). Within this interval, the 18 states are mixtures of singlet and quintet functions, while they are virtually pure quintet or singlet outside this interval. On the other hand, the triplet−quintet crossing, shown at the bottom, is less abrupt and extends over a much wider interval of Fe−L distances. Significant mixture of triplet and quintet functions is observed in the 1.905−1.925 Å interval, introducing the possibility for the system to undergo a change of spin state.

The extremely small singlet−quintet coupling makes the deactivation of the $^1T_1$ states via either $^5T_2$ or ^5E less probable. In addition, the results show no $^1T_1$−$^3T_1$/$^3T_2$ crossing along the symmetric (a_{1g}) stretching coordinate. However, this does not exclude the existence of a singlet−triplet crossing along other Fe−L vibrations. For the present case, there are five other modes that involve Fe−L stretching, namely the e_g and t_{1u} modes. The $e_g(\theta)$ mode implies a simultaneous shortening and elongation of the bonds in the equatorial plane, and the $e_g(\epsilon)$ mode causes the equatorial ligands to be displaced by "a", while the axial ligands are moved by "−2a". The complex is said to be elongated for $a < 0$ and compressed for $a > 0$. Unfortunately, the t_{1u} mode could not be studied. This mode lifts the inversion symmetry, which makes the calculations computationally too demanding. Note that these asymmetric vibrational modes

(62) Hinek, R.; Gütlich, P.; Hauser, A. *Inorg. Chem.* **1994**, *33*, 567–572.

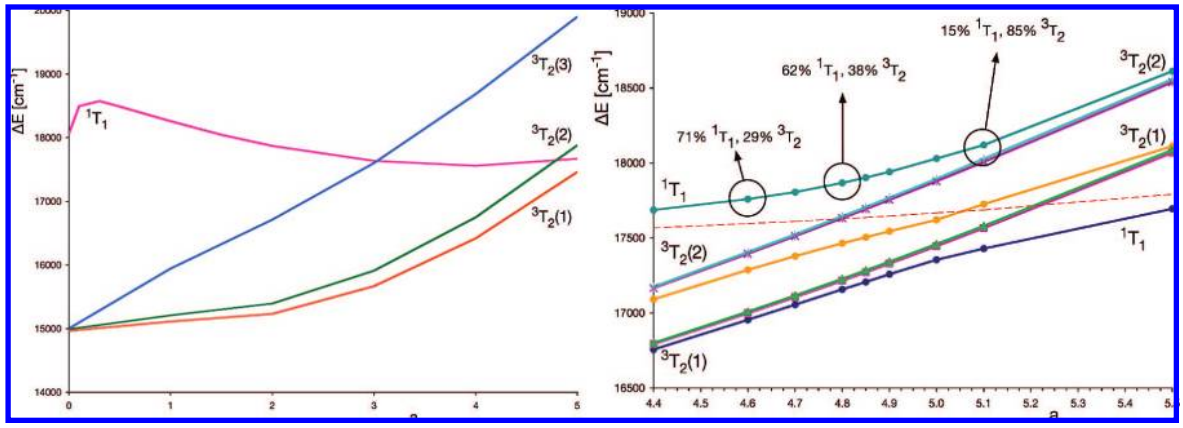

Figure 5. (left) CASPT2 relative energies (cm^{-1}) of the lowest component of the $^1T_1$ state and the three components of the $^3T_2$ state as function of the $e_g(\epsilon)$ vibrational mode. The complex is distorted by moving the equatorial ligands by $+a\Delta r$ and the axial ligands by $-2a\Delta r$ ($\Delta r = 0.01$ Å, the Fe−L distance is 1.94 Å for $a = 0$). (right) Enlargement of the crossing region centered around $a = 4.8$. Spin−orbit resolved relative energies are shown. The dashed line represents the spin-free CASPT2 energy of the $^1T_1$ state.

remove the degeneracy of the three components of the $^3T_2$ state. For convenience, we maintain the same labels to identify the electronic states. While the $^1T_1-^3T_2$ energy difference remains around 3000 cm^{-1} in the $e_g(\theta)$ mode and the elongated complex, we observe a gradual decrease of the triplet−singlet splitting for the compressed complex, leading to two curve crossings. The first occurs at $d(Fe-L)_{eq} = 1.97$ Å and $d(Fe-L)_{ax} = 1.88$ Å, the second, at $d(Fe-L)_{eq} = 1.988$ Å and $d(Fe-L)_{ax} = 1.844$ Å (see Figure 5, left). The spin−orbit coupling between singlet and triplet states in the first crossing is nearly zero, and hence, deactivation via this crossing is unlikely. On the other hand, the effect of spin orbit coupling is significant for the states that cross around 4.8*a* as shown in the right panel of Figure 5. The gradual enlargement of singlet−triplet mixing upon increasing distortion makes possible an intersystem crossing from the excited singlet to one of the components of the $^3T_1$ state.

The observation of a moderate spin−orbit coupling in the singlet−triplet crossing in the compressed $e_g(\epsilon)$ vibrational mode suggest that the LIESST process either involves (i) a singlet → triplet conversion through overlapping excited vibrational levels of the $^1T_1$ and $^3T_2$ and/or $^3T_1$ states or (ii) an intersystem crossing in the asymmetric vibrational mode. Decay by overlap of vibrational levels has recently also been suggested in an experimental study of $Fe^{II}(bpy)_3$ in solution.[63] From the symmetric curves (Figure 3), an estimate of the harmonic vibrational frequency of ∼440 was obtained for the $^1T_1$, $^3T_2$, and $^3T_1$ states so that excited vibrational levels of the triplet state may become close in energy to vibrational levels of the singlet. Moreover, vibrational overlap is favored by the fact that the three curves are nearly parallel to each other. The further deactivation to the HS $^5T_2$ state goes through the $^3T_2-^5T_2$ intersystem crossing at 1.92 Å shown in Figure 4 or the $^3T_1-^5T_2$ intersystem crossing around 1.98 Å. Note that all the conversions take place in a small distance interval in the Franck−Condon region favoring a fast decay of the excited singlet into the metastable HS state.

The curves in Figure 3 suggest that the conversion of the excited quintet state into the LS state of reverse LIESST could be a direct process involving the $^1A_1-^5E$ intersystem crossing at 2.18 Å. However, the small singlet−quintet coupling through spin−orbit interactions makes this route less probable. On the other hand, the ^5E curve also crosses the $^3T_1$ curve close to the equilibrium distance of the $^5T_2$ initial state. Subsequently, the system can relax to the LS state through the $^3T_1-^1A_1$ intersystem crossing at slightly shorter distance.

The analysis of the wave function in terms of valence bond configurations gives additional information about the electronic structure of the compounds under study. Here, we follow the procedure described by Sadoc et al.[64] to obtain atomiclike orbitals and re-express the wave function in these localized orbitals. The HS state in its equilibrium geometry is highly ionic, about 90% of the wave function is due to non-charge-transfer (Fe-$3d^6$) configurations. On the other hand, the wave function of the LS state has a pronounced contribution from LMCT configurations. These Fe-$3d^7L^{-1}$ configurations have a weight of 37% in the wave function. The double CT (Fe-$3d^8L^{-2}$) contribution is 6%, while the rest (56%) arises from the non-charge-transfer configuration.

3.2. Other TM Systems. To analyze the effect of changing the TM on the properties related to the spin crossover phenomenon, we have studied three model systems: $Co^{III}(tz)_6$, $Fe^{III}(tz)_6$, and $Co^{II}(tz)_6$. First, we focus on the Co^{III} complex, which has the same electronic configuration as Fe^{II}, $3d^6$. The upper part of Figure 6 shows the CASPT2 PES for the two lowest singlet, triplet, and quintet states. For this system, the difference between the equilibrium Co-ligand distance (ΔR_{HL}) for the LS (1.90 Å) and the HS (2.05 Å) is shorter than for the $Fe^{II}(tz)_6$ compound, around 0.15 Å. As expected, Co^{III} exerts a stronger field than Fe^{II} leading to a large stabilization of the LS state. Therefore, the bistability between HS and LS disappears, lying the latter more than 15 000 cm^{-1} lower in energy. As a result, no thermal spin crossover can be observed for $Co^{III}(tz)_6$. In order to interpret the character of the HS and LS states, an analysis of the covalency similar to that made for $Fe^{II}(tz)_6$ has been performed. In $Co^{III}(tz)_6$, both states show a more covalent character compared to $Fe^{II}(tz)_6$. For the most stable HS state, the weight of the non-charge transfer configurations in the wave function is around 63% while for the LS state it is only ∼30%, illustrating the larger covalency for the Co^{III} complex. In principle, a weaker σ donor ligand could eventually stabilize the HS state and open the possibility of spin crossover

(63) Gawelda, W.; Cannizzo, A.; Pham, V.-T.; van Mourik, F.; Bressler, C.; Chergui, M. *J. Am. Chem. Soc.* **2007**, *129*, 8199–8206.

(64) Sadoc, A.; Broer, R.; de Graaf, C. *J. Chem. Phys.* **2007**, *126*, 134709.

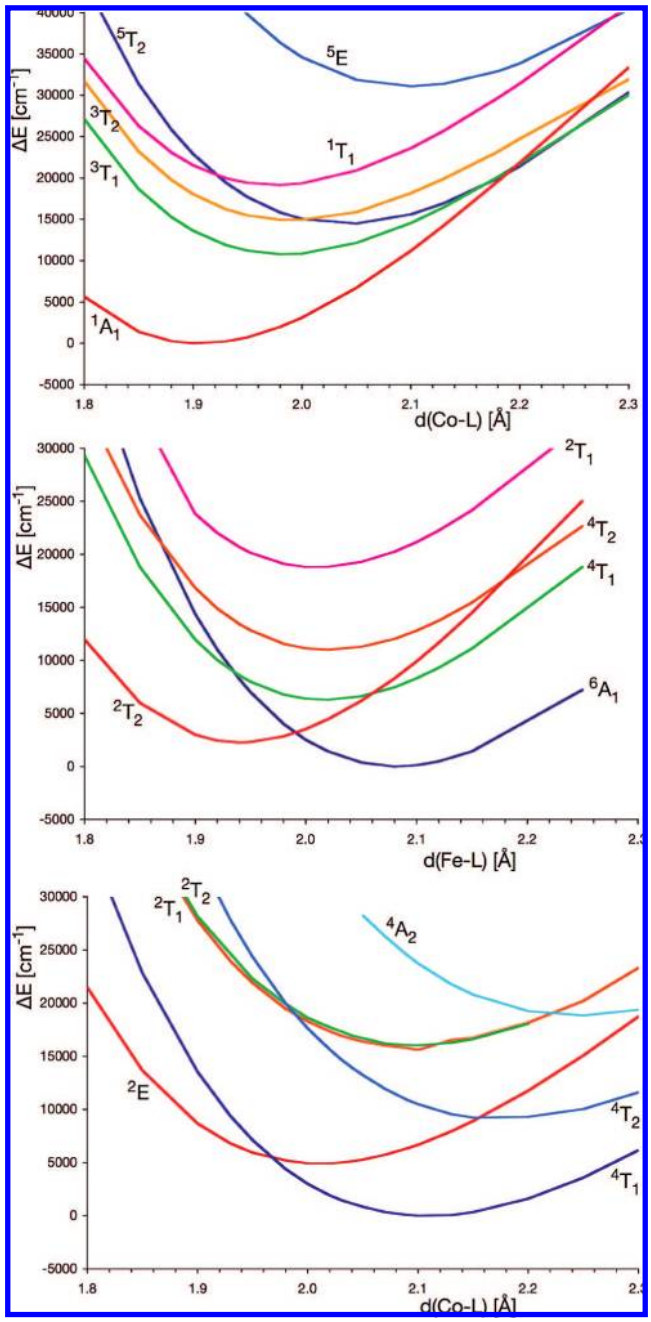

Figure 6. CASPT2 relative energies (cm^{-1}) of the low-lying TM-3d states of $TM(tz)_6$ as function of the TM−L distance. TM = Co^{III} (top), Fe^{III} (middle), and Co^{II} (bottom).

to occur. However, spin crossover Co^{III} complexes are very exceptional and have only been found with F and O coordinating atoms.[65]

We now turn our attention to Fe^{III} systems, for which LIESST has been found in certain coordination compounds. The middle of Figure 6 reports the PES for the lowest electronic states of the $Fe^{III}(tz)_6$ complex. Since the Fe^{III} electronic configuration is $3d^5$, the LS state is a doublet $^2T_2$, the HS a sextet $^6A_1$, and the intermediate spin states are quartets. Both the HS and LS states show more covalent character than the corresponding states in the Fe^{II} system, ∼25% for the HS and almost 70% for the LS state, a similar composition as found for Co^{III} since both TM ions exhibit the same formal oxidation number. In principle, the increased σ-donation should lead to a considerable stabilization of the LS state, in line with the findings for Co^{III} discussed above. However, the HS state of the Fe^{III} ion corresponds to an electronic configuration with a half-filled 3d shell, where the exchange interaction is optimal. The net effect of these two contributions is that the HS electronic state is the ground-state and lies around 1450 cm^{-1} below the doublet LS state. The calculated ΔR_{HL} of 0.14 Å is within the range of values found for spin crossover Fe^{III} complexes. Obviously, for this model system thermal spin crossover is not possible. However, spin-transition phenomenon in Fe^{III} complexes cannot be excluded. In fact, the relatively small energy difference between the HS and LS states could be reversed by substituting the tetrazole ligand for a stronger σ donor. Indeed, spin crossover phenomena in Fe^{III} complexes have been found in a wider range of donor atoms than in Fe^{II}, including chalcogen donor atoms and numerous multidentate ligands.[66] Moreover, other effects not considered in this model system, like cooperative effects may also play a role. The whole profile of the PES shown in Figure 6 for $Fe^{III}(tz)_6$ is similar to that illustrated in Figure 3 for $Fe^{II}(tz)_6$. Consequently, the LIESST process in Fe^{III}-based spin crossover systems may involve similar electronic conversions as in the Fe^{II} compounds discussed in the previous section. The computed HS−LS energy barrier is 3200 cm^{-1}, which is larger than that in the Fe^{II} system. However, this value has to be regarded as an upper limit. In more realistic systems, the curve of the LS state will be stabilized and consequently the barrier will be smaller. The lowest allowed $^2T_2 \rightarrow {}^2T_1$ transition corresponds to an internal Fe^{III} d−d transition and occurs at 18400 cm^{-1} (557 nm), close to the visible light of 550 nm used to induce LIESST effect in some Fe^{III} spin crossover systems.[13] The lowest sextet to sextet electronic transition in the $Fe^{III}(tz)_6$ complex involves a ligand-to-metal charge transfer and the vertical excitation is calculated at higher energy, around 32000 cm^{-1}.

Finally, we consider the $Co^{II}(tz)_6$ compound where Co has a $3d^7$ electronic configuration. The relevant electronic states for this system are doublets and quartets, being the lowest LS state a ^2E and the lowest HS state a $^4T_1$. The character of these states is similar to that found for the Fe^{II} complex because the TM's have the same formal oxidation number. The HS state is mainly ionic, with a covalent contribution of only ∼12% while for the LS state CT effects account for 30%. Figure 6 (bottom) shows the PES of the three lowest doublet and quartet states. The difference in the Co−ligand distance between the HS and LS states is 0.11 Å, in agreement with experimental data.[67] The HS state lies ∼4900 cm^{-1} lower in energy than the LS, in contrast to the $Co^{III}(tz)_6$ system, where the ground-state was LS. This can be explained by the less covalent character of Co^{II} systems. Nevertheless, the LS ^2E state is susceptible to suffer a Jahn−Teller (JT) distortion, which will lead to a stabilization of the LS curve with respect to the HS PES. Indeed, an elongated deformation of the complex was found to stabilize the LS state by ∼3800 cm^{-1} with a Co−ligand equilibrium distance of 2.14

(65) Garcia, Y.; Gütlich, P. In *Spin crossover in Transition Metal Compounds II*; Gütlich, P., Goodwin, H. A., Eds.; Topics in Current Chemistry; Springer-Verlag: Berlin, 2004; Vol. 234, p 49.

(66) van Koningsbruggen, P. J.; Maeda, Y.; Oshio, H. In *Spin crossover in Transition Metal Compounds I*; Gütlich, P., Goodwin, H. A., Eds.; Topics in Current Chemistry; Springer-Verlag: Berlin, 2004; Vol. 233, p 259.

(67) Goodwin, H. A. In *Spin crossover in Transition Metal Compounds II*; Gütlich, P., Goodwin, H. A., Eds.; Topics in Current Chemistry; Springer-Verlag: Berlin, 2004; Vol. 234, p 23.

Å in the axial direction and 1.93 Å in the equatorial plane. Although the HS still lies lower in energy than the JT-distorted LS state, the energy difference between them is fairly small, which opens the possibility of spin crossover if Co^{II} coordinates to a stronger donor ligand.

4. Summary and Conclusions

The structural and electronic properties related to spin crossover phenomena have been studied in a tetrazole-based model compound by means of CASPT2 calculations. The $Fe^{II}(tz)_6$ complex can be considered representative for a large number of Fe^{II} spin crossover systems containing a FeN_6 core. Relevant parameters like the difference in the Fe−ligand distance between the low-spin and high-spin states, the HS−LS energy difference, and the absorption energies are in good agreement with the experimental values measured in similar compounds. The analysis of the potential energy curves of the electronic states involved in the (reverse) LIESST process as function of the Fe−ligand distance enables the interpretation of the LIESST mechanism. From the LS ground state, the $^1T_1$ excited-state is populated by a vertical excitation at ∼18 000 cm^{-1}. There is a $^1T_1-^5T_2$ intersystem crossing in the Franck−Condon region. However, the very small spin−orbit coupling between singlet and quintet states makes this deactivation channel improbable. A direct crossing between the excited singlet and triplet states is not observed along the a_{1g} stretching mode. However, the curves of both states lie rather close in energy and have the same shape with practically equal curvature and Fe−ligand equilibrium distance. Hence, the large vibrational overlap of both electronic states will favor the singlet → triplet conversion. Alternatively, deactivation of the excited singlet to triplet can occur through a crossing along the $e_g(\epsilon)$ vibrational mode. In a second step, the intermediate triplet state decays in the HS state via a $^3T_2-^5T_2$ intersystem crossing. The LS → HS spin transition is expected to be fast since the two electronic conversions take place in the Franck−Condon region. Reverse LIESST takes place by irradiating the system with light of ∼12 000 cm^{-1} inducing a $^5T_2 \rightarrow {}^5E$ transition. The excited HS state decays to the LS state by two intersystem crossings involving an intermediate triplet state, $^5E-{}^3T_1$ and $^3T_1-{}^1A_1$, both allowed by spin−orbit coupling.

The excited states of the tretrazole-based compound discussed here have mainly Fe-$3d^6$ character. The mechanism is however also valid for other Fe^{II} compounds where, depending on the nature of the ligand, excited states may be of ligand-to-metal or metal-to-ligand character. Replacing the central Fe^{II} by Co leads to a drastic stabilization of either the LS state (Co^{III}) or the HS state (Co^{II}). In both cases, ΔR_{HL} decreases significantly. Hence, spin crossover cannot be observed unless the ligand is changed by weaker (Co^{III}) or stronger (Co^{II}) σ donors. In the case of Fe^{III}, the PES are remarkably similar to the Fe^{II} case. The higher formal charge of Fe leads to an increase of the σ-donation, and hence, a stabilization of the LS state. However, this effect is counterbalanced by the increased stability of the HS state due to its half-filled shell electronic configuration leading to an optimal exchange interaction in the 3d-shell. The (reverse) LIESST mechanism in Fe^{III} compounds is therefore expected to involve similar electronic conversion as in the standard case of Fe^{II} compounds.

Acknowledgment. Fruitful discussions with Dr. M. Reguero, Dr. P. J. van Koningsbruggen, and Dr. J. J. Novoa are kindly acknowledged. Financial support has been provided by the Spanish Ministry of Education and Science (Project CTQU2005-08459-C02/BQU) and the Generalitat de Catalunya (2005SGR-00104, 2005SGR-00697, XRQTC).

Supporting Information Available: Validation of the method and energies and cartesian coordinates of $Fe^{II}(tz)_6$LS and HS, $Fe^{III}(tz)_6$LS and HS, $Co^{II}(tz)_6$LS and HS, $Co^{III}(tz)_6$LS and HS, and $Fe^{II}(tz)_6$ $^1T_1$ and $^3T_2(2)$ at the crossing in the $e_g(\epsilon)$ mode around 4.8*a*. This material is available free of charge via the Internet at http://pubs.acs.org.

JA804506H